

Hypervirial Models of Stellar Systems

N. W. Evans[★] & J. An[★]

Institute of Astronomy, University of Cambridge, Madingley Road, Cambridge CB3 0HA, UK

10 March 2019

ABSTRACT

A family of cusped potential-density pairs is introduced for modelling galaxies and dark haloes. The density profile is cusped like $\rho \sim r^{p-2}$ at small radii. The distribution function is simple and takes the form $f \propto L^{p-2} E^{(3p+1)/2}$ (where E is the binding energy and L is the angular momentum). The models all possess the remarkable property that the virial theorem holds locally, from which they earn their name as the *hypervirial family*. Famously, this property was first discovered by Eddington to hold for the Plummer model in 1916. In fact, the seductive properties of the Plummer model extend to the whole hypervirial family, including the members possessing the cosmologically important cusps of $\rho \sim r^{-1}$ or $\rho \sim r^{-3/2}$ or $\rho \sim r^{-4/3}$. The intrinsic and projected properties of the family of models are discussed in some detail.

Key words: celestial mechanics, stellar dynamics – galaxies: structure – galaxies: kinematics and dynamics – galaxies: elliptical and lenticular

1 INTRODUCTION

The allure of spherical models is their simplicity. For sure, there are few exactly spherical galaxies or bulges. But, spherical models are still useful as representations of galactic nuclei, where the kinematics are usually dominated by a central cusp (see e.g., Dehnen 1993; Tremaine et al. 1994). Almost nothing is firmly known about the shapes of the dark matter haloes around disk galaxies. So, it is very reasonable to use spherical models to investigate, for example, the kinematics of distant halo stars and satellite galaxies of the Milky Way (White 1985; Kulessa & Lynden-Bell 1992; Wilkinson & Evans 1999). Globular clusters with long relaxation times, like ω Centauri, roundish dwarf spheroidal galaxies like Draco (e.g., Wilkinson et al. 2002), as well as clusters of galaxies are also possible applications for spherical models.

Plummer set the standard in 1911 when he introduced the model with mass density ρ and potential ψ as a fit to the outer parts of globular clusters;

$$\begin{aligned} \psi &= \frac{GM}{(a^2 + r^2)^{1/2}}, \\ \rho &= \frac{3M}{4\pi} \frac{a^2}{(a^2 + r^2)^{5/2}}. \end{aligned} \quad (1)$$

The real beauty of this model lies in two facts discovered – not by Plummer – but by Eddington in 1916. First, the Plummer model has a very simple distribution function. In fact, Eddington showed that the isotropic distribution function of any spherical model is available immediately as a quadrature (Eddington 1916; Binney & Tremaine 1987, p. 237):

[★] E-mail: nwe, jin@ast.cam.ac.uk

$$f(E) = \frac{1}{\sqrt{8\pi^2}} \left[\int_0^E \frac{d^2\rho}{d\psi^2} \frac{d\psi}{\sqrt{E-\psi}} + \frac{1}{\sqrt{E}} \frac{d\rho}{d\psi} \Big|_{\psi=0} \right]. \quad (2)$$

Here, f is the distribution function, which depends on the binding energy E of the stars alone. Substituting the particular case of the Plummer model, Eddington found the very simple answer

$$f(E) \propto E^{7/2}. \quad (3)$$

Second, Eddington (1916) also pointed out that the isotropic Plummer model has the remarkable property that it obeys the virial theorem locally (of course, any self-gravitating system must obey it globally). At every spot, the kinetic energy in each element ($T = \rho\langle v^2 \rangle/2$) is exactly one-half of the (magnitude of) the local potential energy ($W = -\rho\psi/2$). Therefore, the virial theorem holds ($2T + W = 0$) at each and every spot! Such models we call *hypervirial*.

In this paper, we introduce a new family of cusped galaxy models. Each member of the family has a distribution function that rivals equation (3) in its simplicity. Even more remarkably, each member of the family satisfies the virial theorem locally. The Plummer model is simply the limiting case when there is no cusp.

2 INTRINSIC PROPERTIES

The potential ψ and density ρ of the family of models are

$$\begin{aligned} \psi &= \frac{GM}{(r^p + a^p)^{1/p}}, \\ \rho &= \frac{(p+1)M}{4\pi} \frac{a^p}{r^{2-p}(a^p + r^p)^{2+1/p}}, \end{aligned} \quad (4)$$

where p is a parameter that is a positive real number¹. The case $p = 2$ is recognised as the Plummer model, while the case $p = 1$ corresponds to a model introduced by Hernquist (1990). Generally, the density distribution behaves like $r^{-(2-p)}$ at small radii and falls off like $r^{-(p+3)}$ at large radii. Note that, if $p > 2$, there is a hole at the centre [$\rho(0) = 0$] and the density increases outwards near the centre. The model with $p = \infty$ is a shell of mass M and radius a . Models with $p > 2$ are therefore not astrophysically realistic. Unless otherwise noted, we only consider models for which the parameter p is restricted to lie in the range $0 < p \leq 2$. Henceforth, we use units in which $G = M = a = 1$.

The cumulative mass M_r within the sphere of radius r is

$$M_r = 4\pi \int_0^r \rho r^2 dr = -r^2 \frac{d\psi}{dr} = \frac{r^{p+1}}{(1+r^p)^{1+1/p}} = \frac{1}{(1+r^{-p})^{1+1/p}}, \quad (5)$$

and so the half-mass radius $r_{1/2}$ is

$$r_{1/2} = (2^{\frac{p}{p+1}} - 1)^{-1/p}. \quad (6)$$

The circular velocity curve v_{circ} is

$$v_{\text{circ}}^2 = -r \frac{d\psi}{dr} = \frac{M_r}{r} = \frac{r^p}{(1+r^p)^{1+1/p}}. \quad (7)$$

As $r \rightarrow 0$, the circular velocity tends to zero. As $r \rightarrow \infty$, the circular velocity becomes asymptotically Keplerian. The velocity dispersion is determined by solving the Jeans equation

$$\frac{1}{\rho} \frac{d}{dr} \left(\rho \langle v_r^2 \rangle \right) + 2\beta \frac{\langle v_r^2 \rangle}{r} = \frac{d\psi}{dr}, \quad (8)$$

where β is the Binney's anisotropy parameter $1 - \beta = \langle v_t^2 \rangle / (2\langle v_r^2 \rangle)$, and $\langle v_r^2 \rangle$ and $\langle v_t^2 \rangle$ are the squares of the radial and tangential velocity dispersions. In general, for a given potential-density pair, if the behaviour of β is assumed, then the Jeans equation (8) can be solved using an integrating factor. In particular, if β is a constant, then the radial velocity dispersion becomes

$$\begin{aligned} \langle v_r^2 \rangle &= \frac{1}{r^{2\beta} \rho} \int_{\infty}^r dr r^{2\beta} \rho \frac{d\psi}{dr} \\ &= \frac{(1+r^p)^{2+1/p}}{r^{p-2+2\beta}} \int_r^{\infty} \frac{r^{2p-3+2\beta} dr}{(1+r^p)^{3+2/p}} \\ &= \frac{\psi}{p+4-2\beta} {}_2F_1 \left(\frac{2-2\beta}{p}, -1, 1; \frac{4-2\beta}{p}, 2; -\frac{1}{r^p} \right) \end{aligned} \quad (9)$$

where ${}_2F_1(a, b; c; x)$ is the Gaussian hypergeometric function. In general, $\langle v_r^2 \rangle$ is finite everywhere if $2\beta \leq (2-p)$, while it diverges at the centre if $2\beta > (2-p)$. In fact, An & Evans (2005) show that the models with $2\beta > (2-p)$ are unphysical as the distribution function is not everywhere non-negative.

2.1 Hypervirial Models

It is of course awkward to work with hypergeometric functions, and so it is natural to look for simplifications. Fortunately, a wonderful simplification exists. If $2\beta = (2-p)$ in equation (9), then the hypergeometric function becomes the constant unity! So, the square of the velocity dispersion becomes linearly proportional to the potential everywhere, that is,

$$\langle v_r^2 \rangle = \frac{1}{2p+2} \frac{1}{(1+r^p)^{1/p}} = \frac{\psi}{2(p+1)}$$

¹ The model is a limiting case of the ‘generalized isochronous’ models written down by Veltmann (1979). He however did not study its properties in any detail.

$$\langle v_t^2 \rangle = 2(1-\beta) \langle v_r^2 \rangle = \frac{p\psi}{2(p+1)}. \quad (10)$$

Furthermore, we deduce the unusual result that the total velocity dispersion $\langle v_r^2 \rangle + \langle v_t^2 \rangle = \psi/2$ is independent of p . This leads us to suspect that the distribution functions of these models must also be very simple, though they must be dependent on the angular momentum L as well as the binding energy E since the velocity dispersion tensor is in general anisotropic. It is straightforward to show that if the angular momentum dependence of the distribution function is in the form of a power-law, that is, $f(E, L) = L^{-2\beta} f_E(E)$, then the velocity dispersion anisotropy is everywhere constant and the Binney's parameter becomes the constant β (see e.g., Binney & Tremaine 1987). Motivated by this, we expect the distribution functions of our models will also have the form of $f(E, L) = L^{p-2} f_E(E)$, where $f_E(E)$ is a function of energy that remains to be found.

A little more work shows that $f_E(E)$ is itself a power-law. This follows because the density can be decomposed in terms of a product of powers of the potential and radius

$$\rho = \frac{p+1}{4\pi} r^{p-2} \psi^{2p+1}, \quad (11)$$

and consequently simple distribution functions exist of the form (see e.g., equation B7 of Evans 1994)

$$f(E, L) = CL^{p-2} E^{(3p+1)/2}. \quad (12)$$

Note that $f(E, L = 0)$ diverges for $p < 2$ which is in accordance with the presence of the density cusp at the centre. Here, the constant C can be determined by the normalization condition $\rho = \int f d^3v$ and is

$$C = \frac{1}{2^{p/2+1} (2\pi)^{5/2}} \frac{\Gamma(2p+3)}{\Gamma(p/2)\Gamma(3p/2+3/2)}. \quad (13)$$

Here, $\Gamma(x)$ is the Gamma function. The velocity dispersion tensor is found from the second velocity moments of the distribution function,

$$\begin{aligned} \rho \langle v_r^2 \rangle &= \int v_r^2 f d^3v \\ &= \frac{2\pi C}{r^{2-p}} \int_0^\pi d\theta_v \cos^2 \theta_v \sin^{p-1} \theta_v \int_0^{\sqrt{2\psi}} dv v^{p+2} \left(\psi - \frac{v^2}{2} \right)^{(3p+1)/2} \\ &= \frac{1}{8\pi} r^{p-2} \psi^{2p+2} \end{aligned}$$

$$\begin{aligned} \rho \langle v_t^2 \rangle &= \int (v_\theta^2 + v_\phi^2) f d^3v \\ &= \frac{2\pi C}{r^{2-p}} \int_0^\pi d\theta_v \sin^{p+1} \theta_v \int_0^{\sqrt{2\psi}} dv v^{p+2} \left(\psi - \frac{v^2}{2} \right)^{(3p+1)/2} \\ &= \frac{p}{8\pi} r^{p-2} \psi^{2p+2} \end{aligned}$$

so that

$$\begin{aligned} \langle v_r^2 \rangle &= \frac{1}{8\pi} \frac{r^{p-2} \psi^{2p+2}}{\rho} = \frac{\psi}{2(p+1)} \\ \langle v_t^2 \rangle &= \frac{p}{8\pi} \frac{r^{p-2} \psi^{2p+2}}{\rho} = \frac{p\psi}{2(p+1)} \end{aligned} \quad (14)$$

and

$$\beta = 1 - \frac{\langle v_t^2 \rangle}{2\langle v_r^2 \rangle} = 1 - \frac{p}{2}. \quad (15)$$

When $p = 2$ (the Plummer model), the velocity dispersion is isotropic and the distribution function no longer depends on the

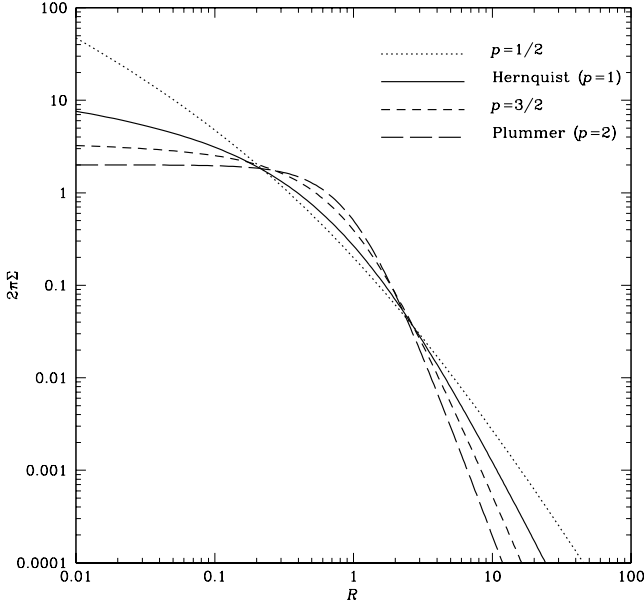


Figure 1. The surface density profile of the hypervirial models with $p = 1/2, 1$ (Hernquist), $3/2$ and 2 (Plummer).

angular momentum. As $p \rightarrow 0$, the density of the models become increasingly cusped and the velocity distribution becomes increasingly dominated by radial orbits.

Note that the kinetic energy T in any element at each point is

$$T = \frac{\rho}{2} (\langle v_r^2 \rangle + \langle v_t^2 \rangle) = \frac{1}{4} \rho \psi = -\frac{W}{2}, \quad (16)$$

where $W = -(\rho \psi)/2$ is the local contribution to the potential energy. In other words, we have established that there exist a virial relation $2T + W = 0$ that holds at every spot. All these models are therefore hypervirial. This generalizes the remarkable result that Eddington (1916) originally found for the Plummer model.

3 PROJECTED QUANTITIES

The beauty of the hypervirial models lies in their simple distributions of velocities. By contrast, the projected quantities are generally more awkward, typically reducing to elementary functions only in the cases of Plummer ($p = 2$) and Hernquist ($p = 1$).

The surface density is

$$\Sigma = 2 \int_R^\infty \frac{\rho r dr}{\sqrt{r^2 - R^2}} = \frac{p+1}{2\pi} R^{p-1} \int_0^{\pi/2} \frac{\cos^{p+1} \theta d\theta}{(R^p + \cos^p \theta)^{2+1/p}}. \quad (17)$$

If the mass-to-light ratio is constant, then this is proportional to the surface brightness. Fig. 1 shows the surface brightness profile for a number of the hypervirial models. For the two special cases, expressions using elementary functions are known (Plummer 1911; Hernquist 1990)

$$\Sigma_P = \frac{1}{\pi} \frac{1}{(1+R^2)^2} \quad \text{Plummer (p=2)}$$

$$\Sigma_H = \frac{1}{2\pi} \frac{1}{(1-R^2)^2} \left[(2+R^2) \frac{\text{arcsech } R}{\sqrt{1-R^2}} - 3 \right] \quad \text{Hernquist (p=1).}$$

Despite the appearance of the formal singularity at $R = 1$ for the $p = 1$ case, Σ_H is in fact regular everywhere for $R > 0$. In particular, it is continuous [$\Sigma_H(1) = (2\pi)^{-1}(4/15)$] and differentiable at $R = 1$.

The central surface density is finite if $p > 1$,

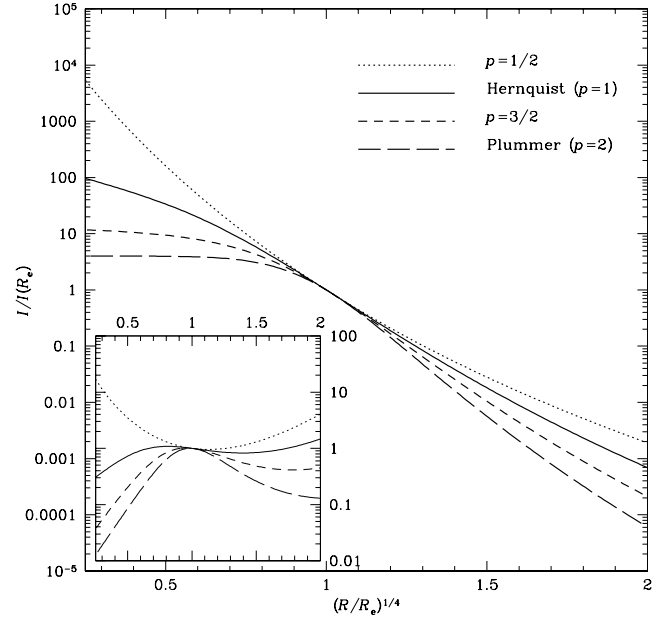


Figure 2. The surface brightness of the hypervirial models with $p = 1/2, 1$ (Hernquist), $3/2$ and 2 (Plummer) plotted against $(R/R_e)^{1/4}$ where R/R_e is the projected distance in units of the effective radius of each model. In this diagram, the de Vaucouleurs (1948) profile would be a straight line with a slope of -3.331 . The inset shows the residuals with respect to the de Vaucouleurs profile.

$$\Sigma(0) = 2 \int_0^\infty \rho dr = \frac{\Gamma(1-1/p)\Gamma(1+2/p)}{2\pi\Gamma(1+1/p)}, \quad (18)$$

but it is divergent otherwise. In particular, if $0 < p < 1$, the central surface density behaves like

$$\Sigma \sim \frac{1}{R^{1-p}} \frac{(p+1)\Gamma(1/2-p/2)}{4\pi^{1/2}\Gamma(1-p/2)} \propto R^{-(1-p)} \quad (R \rightarrow 0), \quad (19)$$

and it diverges logarithmically if $p = 1$ (Hernquist 1990). At large radii, the asymptotic behaviour of the surface density is given by

$$\Sigma \sim \frac{1}{R^{p+2}} \frac{\Gamma(1+p/2)}{2\pi^{1/2}\Gamma(1/2+p/2)} \propto R^{-(p+2)} \quad (R \rightarrow \infty). \quad (20)$$

If the mass-to-light ratio is constant, then the cumulative brightness is proportional to the mass within the cylinder of radius of R , namely

$$\mathcal{M}_R = 2\pi \int_0^R \Sigma R dR = R^{p+1} \int_0^{\pi/2} \frac{\cos \theta d\theta}{(R^p + \cos^p \theta)^{1+1/p}}. \quad (21)$$

For the Plummer and Hernquist models, the result reduces to

$$\mathcal{M}_R^P = \frac{R^2}{1+R^2} \quad \text{Plummer (p=2),}$$

$$\mathcal{M}_R^H = \frac{R^2}{1-R^2} \left(\frac{\text{arcsech } R}{\sqrt{1-R^2}} - 1 \right) \quad \text{Hernquist (p=1).}$$

Note that $\mathcal{M}_R^P(1) = 1/2$ and $\mathcal{M}_R^H(1) = 1/3$. The effective radius (or the half-light radius) R_e can be in general found by numerically solving

$$\mathcal{M}_R(R_e) = \frac{1}{2}.$$

The particular solutions are $R_e \approx 1$ (exact), 1.18084, 1.81527 and 11.0151 for $p = 2, 3/2, 1$ and $1/2$, respectively. Fig. 2 shows the surface brightness normalized by $\Sigma(R_e)$ as a function of $(R/R_e)^{1/4}$.

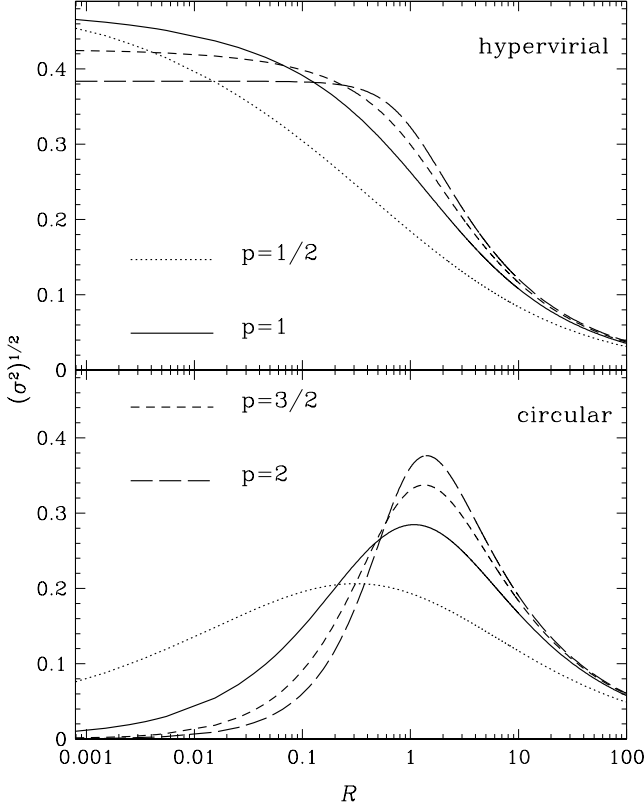


Figure 3. The line of sight velocity dispersion profiles for the hypervirial and circular orbit distribution functions corresponding to the models with $p = 1/2, 1$ (Hernquist), $3/2$ and 2 (Plummer).

We find that Hernquist profile – and by extension the hypervirial models with $p \approx 1$ – are all reasonably good approximations to the empirical de Vaucouleurs $R^{1/4}$ law (1948) of the surface brightness profiles between $0.25 \lesssim (R/R_e) \lesssim 10$. The total mass is of course

$$\mathcal{M}_R(\infty) = \lim_{R \rightarrow \infty} \int_0^{\pi/2} \frac{\cos \theta d\theta}{(1 + R^{-p} \cos^p \theta)^{1+1/p}} = \int_0^{\pi/2} \cos \theta d\theta = 1,$$

as it should be!

For any spherical model with anisotropy parameter β , the line of sight velocity dispersion σ is (e.g., Binney & Tremaine 1987)

$$\Sigma \sigma^2 = 2 \int_R^\infty \left(1 - \beta \frac{R^2}{r^2}\right) \frac{\rho \langle v_r^2 \rangle r dr}{\sqrt{r^2 - R^2}}. \quad (22)$$

For the hypervirial models, $\beta = 1 - (p/2)$ and so

$$\Sigma \sigma^2 = \frac{1}{4\pi} R^{p-1} \int_0^{\pi/2} \frac{\cos^{p+2} \theta + (p/2 - 1) \cos^{p+4} \theta}{(R^p + \cos^p \theta)^{2+2/p}} d\theta. \quad (23)$$

As in the case of the surface density, this integral reduces to elementary functions for the Plummer model

$$\Sigma_P \sigma_P^2 = \frac{3}{64} \frac{1}{(1 + R^2)^{5/2}}; \quad \sigma_P^2 = \frac{3\pi}{64} \frac{1}{(1 + R^2)^{1/2}}$$

and for the Hernquist model

$$\Sigma_H \sigma_H^2 = \frac{1}{4\pi} \left\{ \pi R + \frac{1}{12(1 - R^2)^3} \left[(24R^6 - 68R^4 + 57R^2 - 28) + 3(8R^8 - 28R^6 + 35R^4 - 14R^2 + 4) \frac{\text{arcsech } R}{\sqrt{1 - R^2}} \right] \right\}. \quad (24)$$

This is continuous at $R = 1$ with $\sigma_H^2(1) = [4\pi \Sigma_H(1)]^{-1} [\pi -$

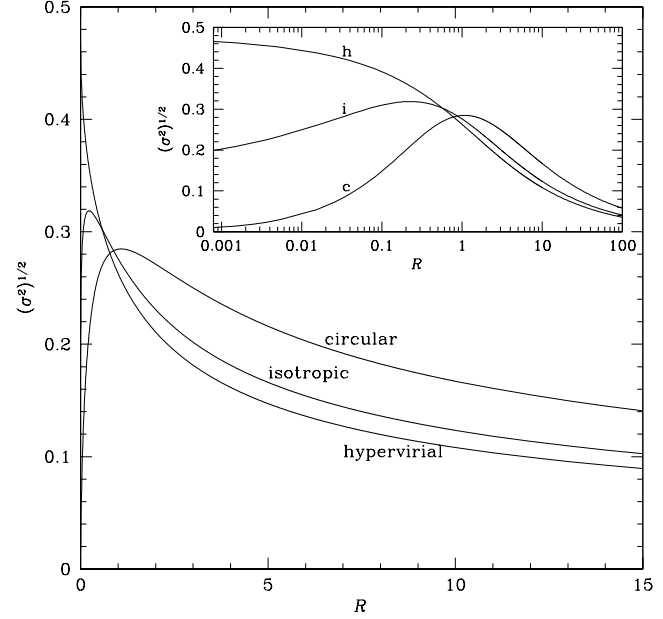


Figure 4. The line of sight velocity dispersion profiles for the isotropic, hypervirial and circular orbit distribution functions corresponding to the Hernquist model (c.f., fig. 1 of Hernquist 1990). The inset is the same but as a function of $\log R$, which shows the behaviour near the centre better.

$(326/105)$]. Note that, the isotropic model was the main object of study of Hernquist (1990) and its line of sight velocity dispersion (eq. 41 of Hernquist 1990) differs from equation (24), of course.

If $p > 1$, then the central value of the velocity dispersion is

$$\sigma^2(0) = \frac{2}{\Sigma(0)} \int_0^\infty \rho \langle v_r^2 \rangle dr = \frac{\Gamma(1 + 3/p)\Gamma(1 + 1/p)}{4\Gamma(2/p)\Gamma(2 + 2/p)}, \quad (25)$$

which varies from $3\pi/64$ for $p = 2$ to $1/4$ as $p \rightarrow 1^+$. On the other hand, if $0 < p < 1$, the central velocity dispersion is

$$\Sigma \sigma^2 \sim \frac{1}{R^{1-p}} \frac{(p+1)\Gamma(1/2 - p/2)}{16\pi^{1/2}\Gamma(1 - p/2)} \sim \frac{\Sigma}{4} \quad (R \rightarrow 0). \quad (26)$$

For the case $p = 1$, using $(1 - R^2)^{-1/2} \text{arcsech } R \sim \ln(2/R)$ as $R \rightarrow 0$, we find that

$$\Sigma_H \sigma_H^2 \sim \frac{1}{\pi} \left(\frac{1}{4} \ln \frac{2}{R} - \frac{7}{12} \right); \quad \Sigma_H \sim \frac{1}{\pi} \left(\ln \frac{2}{R} - \frac{3}{2} \right)$$

$$\lim_{R \rightarrow 0} \sigma_H^2 = \lim_{R \rightarrow 0} \frac{\Sigma_H \sigma_H^2}{\Sigma_H} = \frac{1}{4}.$$

In other word, the line of sight velocity dispersion at the centre is always finite for $0 < p \leq 2$. In particular, $\sigma^2(0) = 1/4$ if $0 < p \leq 1$ while it can be determined from equation (25) for $1 \leq p \leq 2$. At large radii, the fall-off becomes Keplerian

$$\sigma^2 \sim \frac{1}{R} \frac{(p+2)\Gamma(3/2 + p/2)^2}{8\Gamma(3 + p/2)\Gamma(1 + p/2)} \propto R^{-1} \quad (R \rightarrow \infty). \quad (27)$$

It is instructive to compare this with the purely circular orbit model, for which the line of sight velocity dispersion is given by

$$\begin{aligned} \Sigma \sigma^2 &= 2 \int_R^\infty \frac{\langle v_t^2 \rangle R^2}{2} \frac{\rho r dr}{\sqrt{r^2 - R^2}} = R^2 \int_R^\infty \frac{\rho v_{\text{circ}}^2 dr}{r \sqrt{r^2 - R^2}} \\ &= \frac{p+1}{4\pi} R^{2p-1} \int_0^{\pi/2} \frac{\cos^{p+4} \theta d\theta}{(R^p + \cos^p \theta)^{3+2/p}}, \end{aligned} \quad (28)$$

which becomes

$$\Sigma_P \sigma_P^2 = \frac{15}{128} \frac{R^2}{(1+R^2)^{7/2}}; \quad \sigma_P^2 = \frac{15\pi}{128} \frac{R^2}{(1+R^2)^{3/2}} \quad (p=2)$$

$$\Sigma_H \sigma_H^2 = \frac{1}{4\pi} \left\{ \pi R - \frac{R^2}{12(1-R^2)^4} \left[(24R^6 - 92R^4 + 117R^2 - 154) + 3(8R^8 - 36R^6 + 63R^4 - 40R^2 + 40) \frac{\operatorname{arcsch} R}{\sqrt{1-R^2}} \right] \right\} \quad (p=1).$$

Since we only observe radially-directed motion when looking at the very centre, the line of sight velocity dispersion must vanish there for the extreme tangentially anisotropic model. On the other hand, at large radii, we have

$$\sigma^2 \sim \frac{1}{R} \frac{\Gamma(5/2+p/2)\Gamma(3/2+p/2)}{2\Gamma(3+p/2)\Gamma(1+p/2)} \propto R^{-1} \quad (R \rightarrow \infty). \quad (29)$$

By comparing this to equation (27), we find that the line of sight velocity dispersion for the purely circular orbit model is larger than that for the hypervirial model at large radii. This is an expected result, since we observe tangential motion preferentially as the lines of sight moves to the outskirts of the system. In Fig. 3, we plot the line of sight velocity dispersion for the hypervirial and circular orbit model for a few representative values of p . In Fig. 4, the line of sight velocity dispersions for the Hernquist model are shown. The expression for the velocity dispersion of the isotropic model is provided by equation (41) of Hernquist (1990).

4 HYPERVIRIALITY

First, let us ask the question: are there any more spherical models with the property of hyperviriality? Mathematically, such a model has to satisfy

$$\langle v_r^2 \rangle + \langle v_t^2 \rangle = \frac{\psi}{2}. \quad (30)$$

Since $1-\beta = \langle v_t^2 \rangle / (2\langle v_r^2 \rangle)$, if β is constant, equation (30) implies that

$$\langle v_r^2 \rangle = \frac{\psi}{2(3-2\beta)}. \quad (31)$$

On the other hand, the Jeans equation (8) can be written

$$\frac{d\langle v_r^2 \rangle}{dr} + \left[\frac{1}{\rho} \frac{d\rho}{dr} + \frac{2\beta}{r} \right] \langle v_r^2 \rangle = \frac{d\psi}{dr}. \quad (32)$$

From equations (31) and (32), by eliminating $\langle v_r^2 \rangle$, we obtain

$$\frac{d\rho}{dr} = \left[(5-4\beta) \frac{d\ln\psi}{d\ln r} - 2\beta \right] \frac{\rho}{r}. \quad (33)$$

Now, Poisson's equation for a spherically symmetric system reads

$$\frac{1}{r^2} \frac{d}{dr} \left[r^2 \frac{d\psi}{dr} \right] = -4\pi G\rho \quad (34)$$

where the negative sign is due to our choice of the sign for the potential. By eliminating ρ from equations (33) and (34), we can get a third order non-linear differential equation for ψ . However, using the relation $d\psi/dr = \psi(d\ln\psi/dr)$, it is possible to reduce the equation into a second order (non-linear) differential equation for $\chi = (d\ln\psi/dr)$,

$$\frac{d^2\chi}{dr^2} + 2 \frac{d\chi}{dr} \left[\frac{1+\beta}{r} - (1-2\beta)\chi \right] - 2 \left[(1-2\beta)\frac{\chi}{r^2} + (4-5\beta)\frac{\chi^2}{r} + 2(1-\beta)\chi^3 \right] = 0 \quad (35)$$

or additionally changing the independent variable into $t = \ln r$;

$$\frac{d^2\xi}{dt^2} - (1-2\beta)(2\xi+1) \frac{d\xi}{dt} - 2(1-\beta)(2\xi+1)(\xi+1)\xi = 0, \quad (36)$$

where $\xi = (d\ln\psi/d\ln r) = (d\ln\psi/dt)$.

Since equation (36) does not involve the independent variable, its order may be reduced by the substitution (e.g., Ince 1944)

$$\zeta = \frac{d\xi}{dt}; \quad \frac{d^2\xi}{dt^2} = \frac{d\zeta}{dt} = \frac{d\zeta}{d\xi} \frac{d\xi}{dt} = \zeta \frac{d\zeta}{d\xi}$$

so that one finally arrives at

$$\zeta \frac{d\zeta}{d\xi} - (1-2\beta)(2\xi+1)\zeta - 2(1-\beta)(2\xi+1)(\xi+1)\xi = 0. \quad (37)$$

Since this is a first order equation, it is always possible (at least formally) to find an integrating factor, which in this case is

$$I = \frac{1}{[\zeta + \xi(\xi+1)][\zeta - 2(1-\beta)\xi(\xi+1)]}.$$

Then, the equation can be written in the exact form

$$\frac{d}{d\xi} \ln \left[[\zeta - 2(1-\beta)\xi(\xi+1)]^{2(1-\beta)} [\zeta + \xi(\xi+1)] \right] = 0.$$

If $\beta < 1$, we obtain the solution

$$[\zeta - 2(1-\beta)\xi(\xi+1)]^{2(1-\beta)} [\zeta + \xi(\xi+1)] = C \quad (38)$$

where C is constant. If we restrict attention to systems of finite mass, then the potential is asymptotically $\sim 1/r$ and consequently we set $C = 0$ from the boundary condition at $r = \infty$. Then, we find two possible solutions, viz;

$$\zeta = 2(1-\beta)\xi(\xi+1); \quad \zeta = -\xi(\xi+1).$$

Note that the second solution is independent of β . In fact, we find that it leads to vanishing density everywhere so that the second solution is unphysical. For the first solution, we obtain

$$\zeta = \frac{d\xi}{dt} = p\xi(\xi+1); \quad \frac{d\xi}{\xi(\xi+1)} = p dt$$

where $p = 2(1-\beta)$. Then, integrating gives the result that

$$\ln \left| \frac{\xi}{\xi+1} \right| = p(t-t_0); \quad \xi = -\frac{1}{1 \pm e^{-p(t-t_0)}}, \quad (39)$$

where the double sign in front of the exponential appears when the absolute value is removed. However, since $\xi = (d\ln\psi/dt)$, one can integrate equation (39) further to find ψ , that is,

$$\ln \left| \frac{\psi}{\psi_0} \right| = - \int \frac{dt}{1 \pm e^{-p(t-t_0)}} = -\frac{1}{p} \ln \left| 1 \pm e^{p(t-t_0)} \right| \quad (40)$$

so that

$$\psi = \psi_0 \left[1 \pm e^{p(t-t_0)} \right]^{-1/p} = \frac{\psi_0}{[1 \pm (r/r_0)^p]^{1/p}}. \quad (41)$$

Note that the absolute value in equation (40) can be ignored since ψ_0 can be either negative or positive. The solution corresponding to the negative sign in equation (41) is unphysical, while the other solution recovers our hypervirial models. One integration constant ($t_0 = \ln r_0$) corresponds to the scalelength and the other integration constant (ψ_0) becomes the overall scaling factor.

Our original differential equation before reduction was in third order, so we expect the general solution to contain three constants of integration. The hypervirial family is a two-parameter family, and so there exists an additional family of solutions, corresponding to the choice $C \neq 0$ in equation (38) and consequently having either infinite mass or finite extent. Unfortunately, the potential-density pair seems not now to be expressible in terms of elementary functions.

Physically speaking, hyperviriality is related to stability of the model against evaporation. The escape speed is $\sqrt{2\psi}$. In a hypervirial model, the root mean square speed is $\sqrt{\psi/2}$. For any other kind of model, the root mean square speed may lie below the hypervirial value at some places, provided that there is suitable compensation at other places so that the global virial theorem is obeyed. In other words, at some spots, there will be more stars close to the escape speed and hence on the verge of escaping. If a few stars escape by accident or tidal perturbations, then the potential is lowered and stars originally safe would be left with speeds above the escape speed. Hyperviriality therefore aids stability by minimising the number of high-velocity stars.

5 POWER-LAW DISTRIBUTION FUNCTIONS

Now, let us ask the question: are there any more spherical models with simple distribution functions that are just a power of energy multiplied by a power of angular momentum?

Suppose that the distribution function of a spherically symmetric system is indeed given by the ansatz

$$f(E, L) = CL^{-2\beta} E^{n-3/2}, \quad (42)$$

where $\beta < 1$ and $n > 1/2$. Then, the corresponding density becomes

$$\rho = \int f d^3v = 2^{3/2-\beta} \pi^{3/2} C \frac{\Gamma(1-\beta)\Gamma(n-1/2)}{\Gamma(n-\beta+1)} \frac{\psi^{n-\beta}}{r^{2\beta}}. \quad (43)$$

The velocity dispersions may also be found as

$$\begin{aligned} \langle v_r^2 \rangle &= \frac{1}{\rho} \int v_r^2 f d^3v = 2^{3/2-\beta} \pi^{3/2} C \frac{\Gamma(1-\beta)\Gamma(n-1/2)}{\Gamma(n-\beta+2)} \frac{\psi^{n-\beta+1}}{\rho r^{2\beta}} \\ &= \frac{\psi}{n-\beta+1} \end{aligned}$$

$$\begin{aligned} \langle v_t^2 \rangle &= \frac{1}{\rho} \int (v_\theta^2 + v_\phi^2) f d^3v = 2^{5/2-\beta} \pi^{3/2} C \frac{\Gamma(2-\beta)\Gamma(n-1/2)}{\Gamma(n-\beta+2)} \frac{\psi^{n-\beta+1}}{\rho r^{2\beta}} \\ &= \frac{2(1-\beta)\psi}{n-\beta+1}. \end{aligned} \quad (44)$$

However, the total kinetic energy T is

$$\begin{aligned} T &= \frac{1}{2} \int \rho (\langle v_r^2 \rangle + \langle v_t^2 \rangle) d^3r = \frac{1}{2} \int d^3r \rho \frac{(3-2\beta)\psi}{n-\beta+1} \\ &= -\frac{3-2\beta}{n-\beta+1} W \end{aligned} \quad (45)$$

where W is the total potential energy. In other words, the sum $W + 2T$ is

$$W + 2T = \left[1 - \frac{2(3-2\beta)}{n-\beta+1} \right] W = \frac{n+3\beta-5}{n-\beta+1} W, \quad (46)$$

suggesting that the global virial theorem for a steady state system is satisfied only if $n+3\beta=5$ [or, in other words, if $\beta=1-(p/2)$, then $n=2+(3/2)p$ and $n-3/2=(3p+1)/2$]. In this case, the total potential energy can be explicitly evaluated as

$$W = -2T = -2\pi \int_0^\infty \rho \psi r^2 dr = -\frac{\pi^{1/2}}{2^{2/p+2}} \frac{\Gamma(1/p+2)}{\Gamma(1/p+3/2)} \quad (47)$$

where $p=2(1-\beta)=2(n-2)/3$. So, our hypervirial models are the only spherically symmetric steady-state systems with finite mass which have distribution functions as simple as equation (42). In particular, the density profile of the Plummer model is the only spherically symmetric self-gravitating polytrope of finite mass with an infinite extent that can be thermally (pressure) supported.

There are other spherical models known which do have distribution functions as simple as equation (42) – namely, the power-law spheres (Evans 1994). However, these models have infinite mass and so do not satisfy the global virial theorem (unless boundary terms are added). Similarly, stellar dynamical polytropes also exist, but have distribution functions $f \propto (E - E_0)^N$, where E_0 and N are constants (Eddington 1916). Only for the Plummer model does E_0 vanish and so the model is of infinite extent.

6 CONCLUSIONS

This paper has provided a set of very simple distribution functions for a family of cusped spherical galaxy models. If the density is cusped like $\rho \sim r^{p-2}$ at small radii, then there is a simple anisotropic distribution function, which behaves like $f \propto L^{p-2} E^{(3p+1)/2}$ (where E is the binding energy and L is the angular momentum). We call these models the hypervirial family. This is because every model obeys the virial theorem at each and every spot, as well as of course globally.

The family includes the Hernquist model which possesses the cosmologically important $1/r$ cusp at small radii and has a simple distribution function $f \propto L^{-1} E^2$. As its sole isotropic and uncusped representative, the family includes the Plummer model with its familiar distribution function $f \propto E^{7/2}$. There are also members which possess other density cusps like $\rho \sim r^{-4/3}$ and $\rho \sim r^{-3/2}$, which have been suggested as important on cosmogonic grounds (Evans & Collett 1997; Moore et al. 1998).

In a sense, the models in this paper really are the last word in simplicity – for we have proved that they are the only self-gravitating, spherically symmetric finite mass models with such simple distribution functions.

REFERENCES

- An J.H., Evans N. W., 2005, ApJ, submitted (astro-ph/0501092)
- Binney J., Tremaine S., 1987, Galactic Dynamics. Princeton University Press, Princeton
- Dehnen W., 1993, MNRAS, 265, 250
- de Vaucouleurs G., 1948, Ann. d’Astrophys., 11, 247
- Eddington A. S., 1916, MNRAS, 76, 572
- Evans N. W., 1994, MNRAS, 267, 333
- Evans N. W., Collett J. L., 1997, ApJ, 480, L103
- Hernquist L., 1990, ApJ, 356, 359
- Ince E. L., 1944, Ordinary Differential Equations. Dover, New York
- Kulessa A., Lynden-Bell D., 1992, MNRAS, 255, 105
- Moore B., Governato F., Quinn T., Stadel J., Lake G., 1998, ApJ, 499, L5
- Plummer H. C., 1911, MNRAS, 71, 460
- Tremaine S. D., Richstone D. O., Byun Y., Dressler A., Faber S. M., Grillmair C., Kormendy J., Lauer T. R., 1994, AJ, 107, 634
- Veltmann Ü.-I. K., 1979, Astron. Zh., 56, 976
- Wilkinson M. I., Evans N.W., 1999, MNRAS, 310, 645
- Wilkinson M. I., Kleyna J., Evans N.W., Gilmore G., 2002, MNRAS, 330, 778
- White S. D. M., 1985, ApJ, 294, L99